16th World Conference on Earthquake Engineering, 16WCEE 2017
Santiago Chile, January 9th to 13th 2017
Paper N° 82SS (Abstract ID)
Registration Code: S- M1452365473

DETERMINISTIC AND PROBABILISTIC ASSESSMENT OF EARTHQUAKE HAZARD FOR THE ISTANBUL METROPOLITAN AREA

P. Gülkan[(1)]

[(1)] *Civil Engineering Program, Middle East Technical University, Northern Cyprus Campus, Güzelyurt, TRNC, pgulkan@metu.edu.tr*

Abstract

Earthquakes that might plausibly nucleate in the westernmost part of the North Anatolian Fault Zone are the events that would serve as arbiters of the ground motions to be experienced in the extended area of Istanbul, the largest city in Turkey. The consequences of a destructive earthquake in the Sea of Marmara region would be enormous for the country. The continued focus on the estimate of the regional seismic hazard is based on this fact. In engineering applications, probabilistic or deterministic approaches for seismic hazard assessment may have precedence over one another depending upon how well quantified their parameters are. Using both approaches, estimates for peak values of ground-motions are made for the Istanbul metropolitan area. In the deterministic approach, six plausible earthquake scenarios are developed. These scenarios consist of individual and multiple rupturing of the submarine fault segments along the western part of the North Anatolian Fault Zone (NAFZ) extending into the Sea of Marmara. The probabilistic approach uses two different earthquake source models: (1) the smoothed-gridded seismicity model and (2) fault model. Alternate magnitude-frequency relations are used. The regional exposure is mapped on a set of hazard maps where a suite of appropriately selected ground motion prediction equations (GMPEs) have been used in a combinatorial approach to address epistemic uncertainty. In lieu of subjectively weighting the expressions, the GMPEs are weighted proportionally, with regard to their relative performance in predicting the measured peak ground motions of the 1999 M7.4 Kocaeli earthquake when it ruptured the Izmit segment of the NAFZ up to the eastern reaches of Istanbul. This computational approach has resulted in consistent but different weights for each GMPE at different spectral periods. High-resolution (0.002 deg by 0.002 deg, or approx. 250 m by 250 m) seismic hazard maps that incorporate site amplification due to softer sediments, provide peak horizontal ground acceleration (PGA) and spectral acceleration values at 0.2, 0.3, 0.5, 1, 1.5, 2, 3 and 4 s.

Keywords: hazard assessment; Istanbul; North Anatolian Fault Zone; soil effects

1. Introduction

To the extent that ground motion contours of future earthquakes can be drawn in scientifically defensible ways on the basis of what we understand of the chaotic processes that take place within the earth, seismic hazard maps serve as useful guides for engineering applications and planning tools. Natural disasters never repeat themselves in all of their fine details, so an earthquake that occurred two hundred years ago will not leave the same imprint in terms of the ground motion that the built environment will experience. Estimating the order-of-magnitude values of those effects is still an invaluable component of disaster preparedness. Estimating earthquake ground motions can be done in accordance with procedures that have been developed along two complementary paths. These are the specific steps embodied in the deterministic and probabilistic approaches. The results should ideally be in large measure in agreement.

This paper discusses the results of that exercise performed for the Istanbul metropolitan area, which comprises the most parts of the northern shores of the Sea of Marmara.

2. Backdrop

Twenty-four centuries ago, probably at about the time when small human settlements had first emerged in what is recognized today as Istanbul, Aristotle said: “Experience shows that a very populous city can seldom, if ever, be properly governed.” We do not know if he had seismic risk management in mind. His notion of a populous city and its governance were arguably much different from what we today understand from those words. Recent findings have pushed the age of the city by another six millennia, but a precise age determination is not relevant. By any measure of quantification, Istanbul today qualifies as the true metropolitan heart of Turkey: population, areal extent, size and volume of financial and industrial services sector, transportation hub, concentration of educational, industrial and media establishments and its historic heritage. Recurrence of one of those major historic earthquakes might herald a disastrous natural disaster for the city.

Istanbul is at seismic risk. The city has been visited by well-recorded severe earthquakes in the past, and experienced destruction. The moment magnitude (M) 7.4 earthquake that occurred in Kocaeli and Sakarya provinces to the east in 1999 was centered some 80 km from the historic city core, but several recently developed districts lying to the west of the city witnessed residential building collapses and life loss. There is a reason to expect that the segment of the North Anatolian Fault traversing the Sea of Marmara at about 15-20 km south of the city proper may rupture in the near future, causing damage in buildings, modern as well as historic (Parsons et al. 2000; Parsons, 2004; Griffiths et al., 2007). During the last 2000 years, 55 documented major earthquakes have occurred in the Marmara Sea region. Many have caused severe damage (Finkel and Ambraseys, 1997; Mazlum, 2003, Ambraseys, 2009). Istanbul sits astride the 30 km-long eponymous strait that connects the Black Sea with the Sea of Marmara (left frame in Fig. 1). An engraving from the 16th century shows the Historic Peninsula from the east in the right frame of the same figure. The walled city was then separated from a smaller settlement on the north side of Haliç, an estuary known also as the Golden Horn.

Viewed through the seismological prism, Istanbul has never been the placid metropolis that these images would suggest. It is in fact under grave danger to be revisited by an earthquake similar to one of the historic events that occurred nearby. This paper deals with ongoing research (e.g., Kalkan et al., 2009) aimed at understanding the hazard better through several (imperfect) instruments (Gülkan, 2013) that are used in current practice.

2.1 Context

The devastating 1999 Kocaeli (M7.4) and Düzce (M7.2) earthquakes on the North Anatolian Fault Zone (NAFZ) on the south of the eastern border of Istanbul province are the most recent manifestation of this high seismic activity. The 1,200 km long NAFZ has a transform mechanism, and runs across northern Turkey accommodating a ~25 mm/year right-lateral slip between Anatolia and the stable Eurasian plates (Straub et al.,1997; McClusky et al., 2000). Since 1939, this fault system has produced ten M≥6.7 earthquakes in a westward-propagating sequence (Fig. 2). Based on the stress transfer postulate for successively rupturing fault segments, and confirmed by the city’s sequenced history of destructive earthquakes, Istanbul is considered likely to experience a major

Fig. 1- View of Istanbul Strait (left), and historic engraving showing the Historic Peninsula (right).

earthquake during the next few decades (Parsons, 2004). This is considered to be a convincing postulate: the seismic hazard for Istanbul metropolitan area is mostly due to submarine fault system at the western extension of NAFZ located south and southeast of Istanbul (Islands and Çınarcık fault segments) and southwest of the city (Mid-Marmara and Off-Tekirdağ fault segments) (Le Pichon et al., 2001; Armijo et al., 2002; Le Pichon et al., 2003; Armijo et al., 2005). This fault system has been recognized to have the potential to nucleate a M≥7 event, which will strongly shake the Istanbul metropolitan area and its surroundings. Its last significant movement of the same order of magnitude as is now forecast has occurred in 1766, so it may well be primed now to rupture again. The stage is thus set: the country's and city's administrators must develop an action plan to mitigate what that earthquake will engender. Its citizens and government must brace for it.

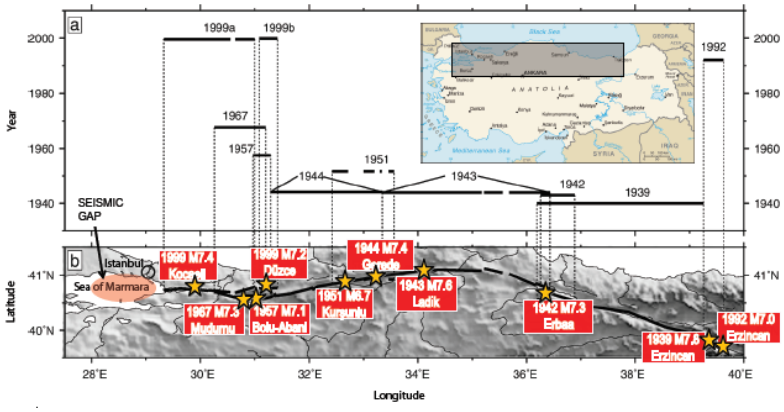

Fig. 2 - Sequence of westerly propagating ten large (M≥6.7; M=moment magntidue) earthquakes on the North Anatolian Fault Zone (NAFZ), shown with thick black line. Potential seismic gap in the Sea of Marmara is highlighted; also shown are the fault rupture length for each event along the NAFZ; the most recent events of this sequence are the 1999 M7.4 Kocaeli (Izmit) and M7.2 Düzce earthquakes. (Figure has been adopted from Kalkan et al., 2009)

Two fault systems located south and southeast of Istanbul (Yalova fault segment and the Northern boundary fault) have the potential to rupture (Parsons et al., 2000; Hubert-Ferrari et al., 2000). Based on renewal model, the probability of occurrence of M7.0 and greater earthquakes in the Marmara region, which could directly influence the Istanbul Metropolitan area was computed as 44±18% in the next 30 years (Parsons, 2004). Marmara region has a complex and heterogeneous fault system as shown in Fig. 3. The 1200 km long NAF system extends from the east of the region towards to the Bay of Izmit. In the east at the junction of the Marmara Sea, NAF system is controlled by right-lateral strike-slip faults, while the plate boundary changes into a trans-tensional system that has opened a deep-basin below the Marmara Sea (Okay et al., 2000). There is no evidence

of a single, continuous, purely strike-slip fault under the Marmara Sea, but a complex segmented fault system with large normal components identified from seismic reflection surveys. In the past a series of strong earthquakes have ruptured the NAF zone in this region. Kocaeli and Düzce events were the latest in a westward-propagating earthquake sequence on this fault system that began with the M7.9 Erzincan earthquake in 1939. This progression has since generated nine M≥7 earthquakes. When the 1912 event (Fig. 3) that occurred in the west of the Marmara Sea is taken into account, a seismic gap that has not ruptured for more than 200 years is identified. This crosses close to the northern shoreline of the Marmara Sea and is around 150-160 km long. It has the potential to generate a M>7.0 earthquake (Hubert-Ferrari et al., 2000). Preliminary calculations show that positive stress changes in the aftermath of the 1999 Kocaeli earthquake on the fault segments below the sea may indicate their likely impact on the rupture potential (Parsons et al., 2000).

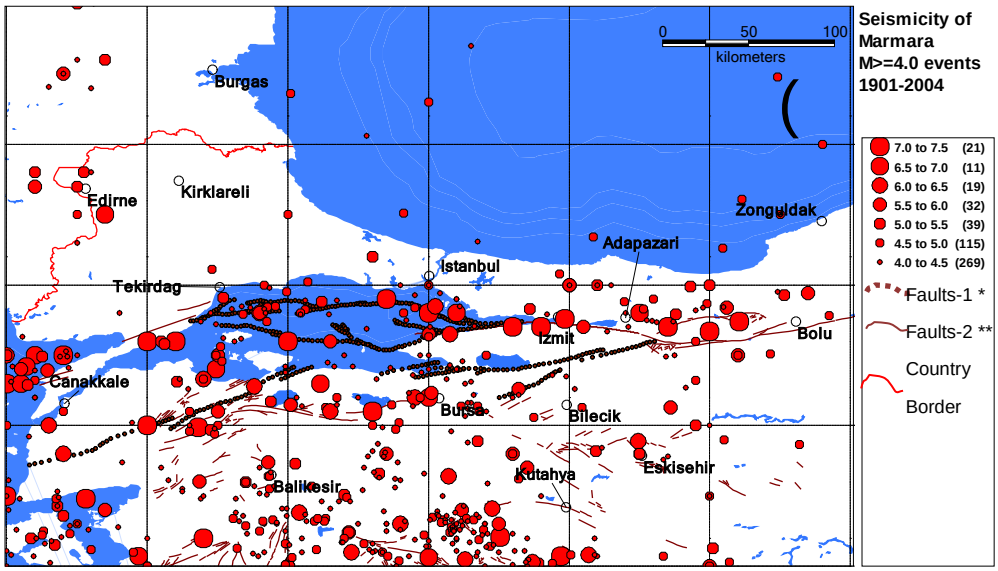

Fig. 3 - Active faults in the Marmara region. The map shows also the 103-year seismicity (between 1901 and 2004) of the region. Parentheses denote the magnitude breakdown of earthquakes.

2.2 Earthquake Catalog

The earthquake catalog includes events from historical and instrumental seismicity. The magnitude, epicenter coordinates and depth of all events with M ≥ 6.0 were considered. The events were compiled from different sources: Earthquake Research Department, General Directorate of Disaster Affair of Turkey, Kandilli Observatory, Boğaziçi University, International Seismological Center of UK, and United States Geological Survey. Magnitude scales of all events were converted to moment magnitude through a set of empirical equations derived based on Turkish earthquakes (Yenier et al., 2008).

3. Ground Motion Prediction Equations

Seismic engineering design hinges on ground motion intensity expressed in terms of estimated spectral acceleration. That estimate is based on ground-motion prediction equations (GMPEs) that have been derived from recordings at strong motion stations. They consider a variety of magnitudes, faulting types, distances, and local soil conditions. Derivation of GMPEs has become a major area of activity for engineering seismology research. Like most estimates that have been developed from intricate use of statistics each new earthquake that yields new recordings provides equal measure of confirmation or refutation of existing GMPEs. In the post-1999 period, many ground-motion records were retrieved in Turkey. This body of new data was combined with existing national ground-motion library to develop a GMPE to be used for regional hazard assessments (Gülkan and Kalkan, 2002). This model was updated later considering a larger data set (Kalkan and Gülkan, 2004a,b). There exist more recent GMPEs that have been derived from other sources, e.g., Akkar et al. 2009. In the study

presented herein, three Next Generation Attenuation (NGA) relationships (Campbell and Bozorgnia, 2008; Boore and Atkinson, 2008; Chiou and Youngs, 2008) were used in addition to the GMPE of Kalkan and Gülkan (2004) to compute the ground motions at distances less than 200 km. I compared the attenuation curves based on four different GMPEs for PGA, spectral acceleration (SA) at 0.2 sec, and 1.0 sec for a M7.0 event on a strike-slip fault and site condition is firm rock (V_{S30} = 760 m/sec) in Fig. 4. The three NGA relationships produce similar results in between themselves. For PGA and SA at 0.2 sec, Kalkan and Gülkan (2004) yields slightly lower acceleration values at closer and farther distances (within 5 km of fault rupture and distances larger than 25 km), whereas its predictions are larger in the intermediate distances (between 5 to 25 km). For SA at 1.0 sec, it estimates larger acceleration values at almost all distances as compared with Boore and Atkinson (2008) and Campbell and Bozorgnia (2008). Chiou and Youngs (2008) yields the highest accelerations at distances less than 5.0 km. Beyond this curve, it under-predicts Kalkan and Gülkan. Except for Chiou and Youngs, the other three GMPEs' predictions seem to merge at distances less than 1.0 km (Fig. 4).

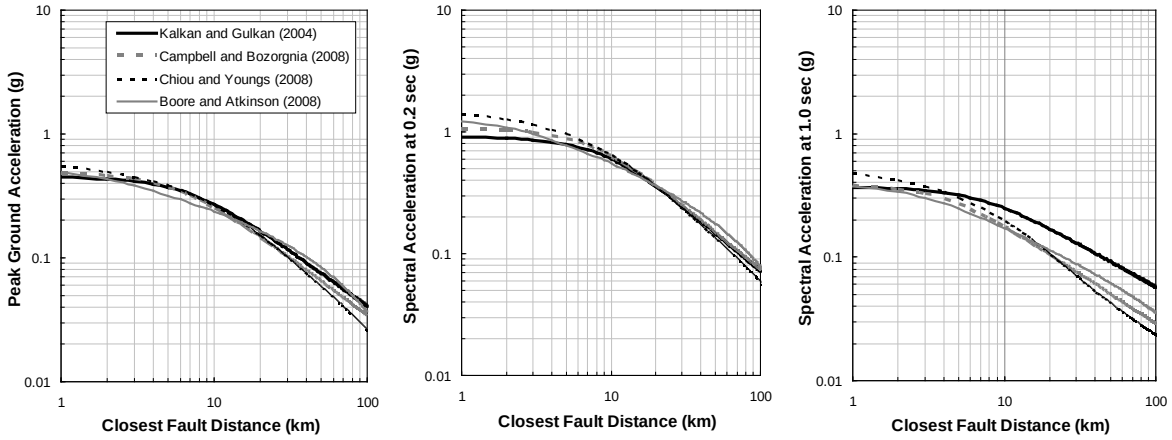

Fig. 4 - Comparisons of ground motion predictions from Kalkan and Gülkan (2004) ground-motion prediction equation with three next-generation attenuation relations (Boore and Atkinson, 2008; Campbell and Bozorgnia, 2008; Chiou and Youngs, 2008). Plots are for peak ground acceleration (left panel) and spectral acceleration (SA) at 0.2 sec (middle-panel) and 1.0 sec (right panel). Ground motion prediction is based on an assumed moment magnitude 7.0 event on a strike-slip fault (with depth of 2 km) and on uniform firm rock (engineering rock) site condition (V_{S30} = 760 m/s).

Instead of a subjective assignment, logic-tree weights of competing GMPEs were determined according to their relative performances in predicting observed ground motions of the 1999 M7.4 Kocaeli earthquake. This non-subjective computational approach led to each GMPE having varying logic tree weights at each spectral period. Not surprisingly, this analytical approach resulted in slightly larger weight for the Kalkan and Gülkan (2004) expression at all periods of interest because it is based precisely on that one event. A GMPE providing a smaller overall standard deviation of prediction among other GMPEs is weighted more. The relative weights of GMPEs for each intensity measure (IM) (that is, PGA or spectral accelerations at *T*) is calculated as follows:

1) Compute the residuals for the i^{th} GMPE; residuals correspond to the difference between the observations and predictions in natural-log space,
2) Using the residuals, compute standard deviation of prediction, σ_i for the i^{th} GMPE,
3) Relative weight, W_i, for the ith GMPE is computed as $W_i = \left[1/\sigma_i^2\right] / \left[\sum_{i=1,n}(1/\sigma_i^2)\right]$ where *n* is the total number of GMPEs selected.

4. Hazard: Probability Based Estimates

The seismic hazard is computed for PGA and SA ordinates at 0.2 and 1.0 sec for the uniform firm rock site condition (V_{S30} = 760 m/sec). The 0.2 and 1.0 sec spectral periods are selected because they are frequently used to construct a smooth design spectrum. Seismic hazard for the Marmara region was computed for maximum credible earthquake level—2 and 10% probabilities of being exceeded in 50 years corresponding to 2475 and 475 year return period. In Figures 5 through 8, the mean seismic hazard computed for PGA, SA at 0.2 sec, and 1.0 sec for these probability levels. The distribution of PGA and SA ordinates, shown by the color gradient, indicates a broader scattering of higher acceleration values toward the south and east of the Marmara region because the faults segments and their scatter that dominates the seismic activity in the eastern section are greater than in the western section of the region. For the 2475 year return period, maximum PGA (Fig. 5) at a firm rock site is computed as 1.5 g. It diminishes to 0.8 g for 475 years. Such high values of PGA are observed in the vicinity of fault segments along the branch of the NAF zone extending into the Sea of Marmara. This zone of large ground motions also correspond to areas where large numbers of M4+ events have occurred since 1901. At the same locations, the maximum SA at 0.2 sec (Fig. 6) is computed as 2.8 g and 1.8 g at the return periods of 2475 and 475 years, respectively. The maximum SA at 1.0 sec (Fig. 7) is computed as 1.5 g for 2475 year return period and 0.8 g for 475 year return period.

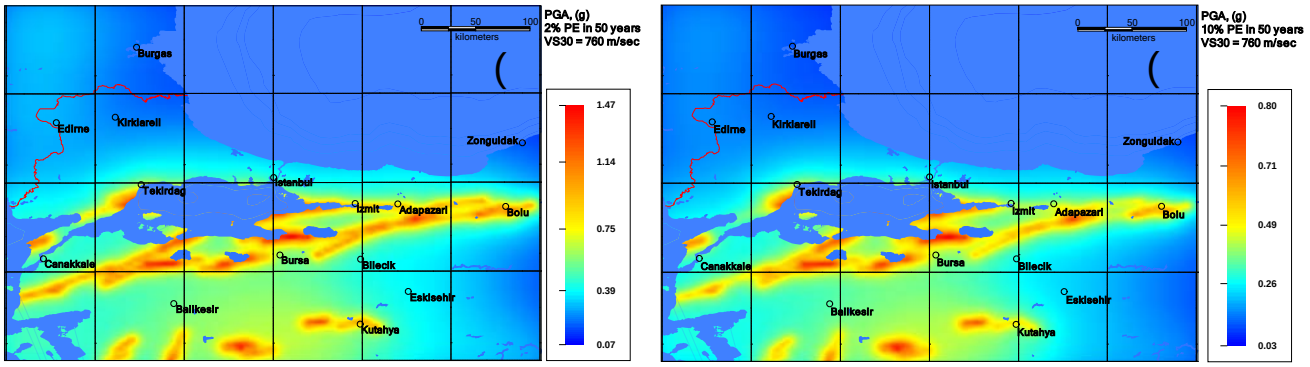

Fig. 5 - Seismic hazard in the Marmara region for peak ground acceleration (PGA) for uniform firm rock site condition for 2% (left panel) and 10% (right panel) probability of being exceeded in 50 years. Grid spacing is 1°; latitude and longitude of left upper corner of each map are 43° N and 26° E.

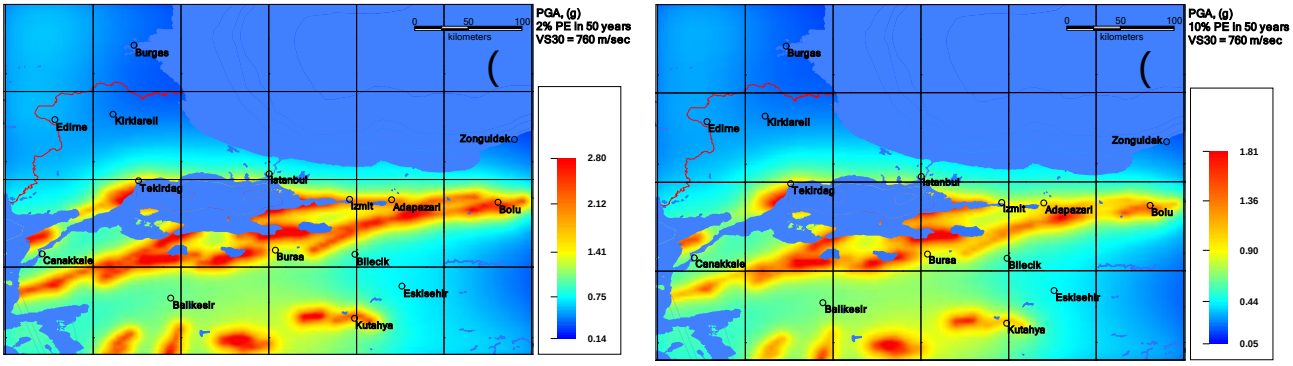

Fig. 6 - Seismic hazard in the Marmara region for spectral acceleration (SA) at 0.2 s for uniform firm rock site condition for 2% (left panel) and 10% (right panel) probability of being exceeded in 50 years. Grid spacing is 1°; latitude and longitude of left upper corner of each map are 43° N and 26° E.

The hazard maps presented in Figures 5 through 7 are for a uniform firm rock site condition. To obtain motion estimates for average soil site (V_{S30} = 360 m/s) and soft-soil site (V_{S30} = 180 m/s), the mapped values should be modified. It is not possible to provide a constant modification factor to transfer the hazard values computed for V_{S30} = 760 m/sec to those at V_{S30} = 360 m/sec or 180 m/sec because the three NGA relations have nonlinear site

correction term, i.e., site amplification increases with decrease in ground motion intensity at least for PGA, SA at 0.2 sec, and 1.0 sec for soil and soft-soil sites (Choi and Stewart, 2005). Unlike the NGA relations, Kalkan and Gülkan (2004) GMPE uses a linear site correction term. In order to predict the ground motion at soil and soft-soil sites, we computed the amplification factors at every grid point and projected them on a series of site amplification maps in Figures 8 through 10. These maps are generated for PGA and SA at 0.2 sec and 1.0 sec considering ground motion level for the ubiquitous number of 2475 years.

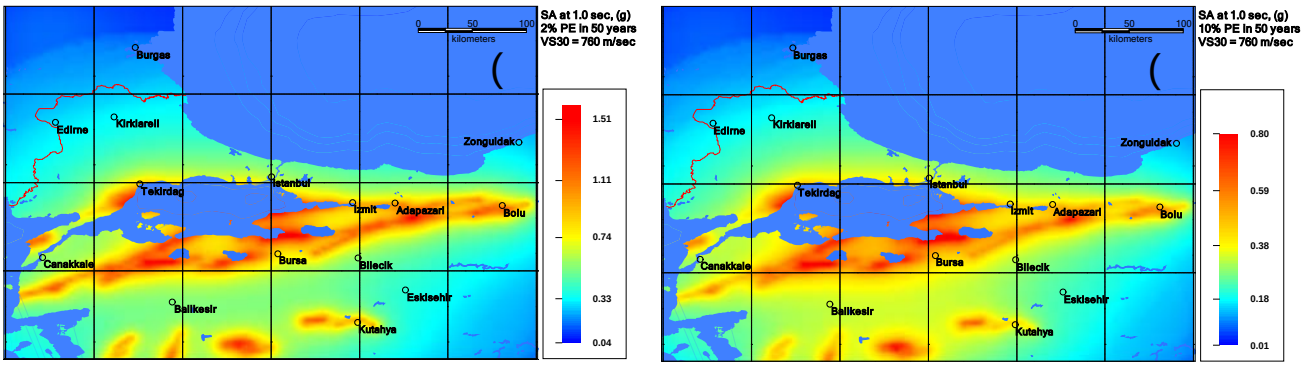

Fig. 7 – Seismic hazard in the Marmara region for spectral acceleration at 1.0 sec for uniform firm rock site condition for 2% (left panel) and 10% (right panel) probability of being exceeded in 50 years. Grid spacing is 1°; latitude and longitude of left upper corner of each map are 43° N and 26° E.

Site amplification factors for V_{S30} = 180 m/sec are almost unity at the locations where the high PGA values are computed (Fig. 8). For V_{S30} = 180 m/sec, Kalkan and Gülkan (2004) yields a constant amplification factor of 1.3 independent of the PGA level. For PGA of 0.3 g and higher, NGA relations yield site amplification factors less than unity, therefore combination of the four GMPE within the logic tree results in "no site amplification" around the major fault lines. The same applies for SA at 0.2 s (Fig. 9). However, for SA at 1 s, NGA relations yield amplification factors greater than unity, thus soft-soil sites around the major fault lines are expected to experience a minimum 1.6 times higher ground motion as compared to the uniform firm rock sites (Fig. 10). While the results reflect the particular traits of the GMPEs that have been used to generate them, they provide a pointer for how unreasonably elevated values close to faults can be brought under "control" because of the singular nature of some GMPEs for zero distance. An arguable presumptuous way of shaving uncomfortable peaks in the strips alongside active faults was practiced for the proposed seismic hazard map for Turkey.

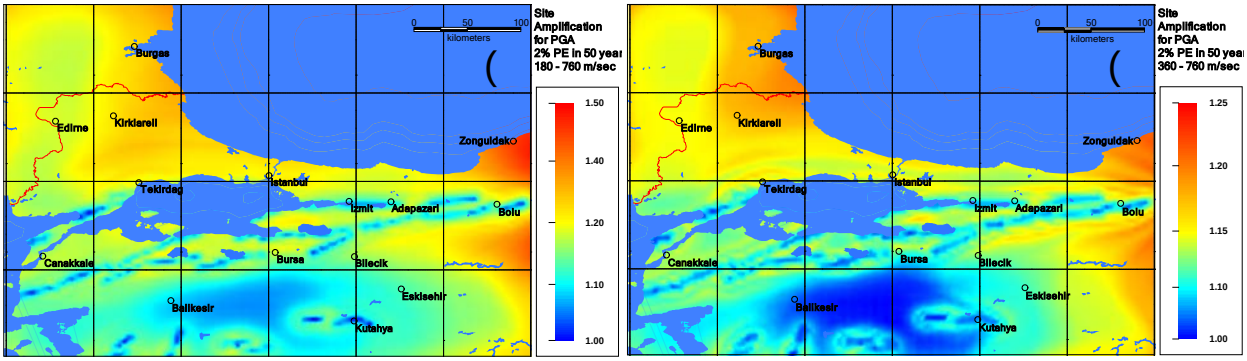

Fig. 8 - Site amplification map of the Marmara region for PGA for 2% probability of being exceeded in 50 years. Left panel shows ratio of ground motion estimate between V_{S30} = 180 m/sec and V_{S30} = 760 m/sec; right panel shows ratio of ground motion estimate between V_{S30} = 360 m/sec and V_{S30} = 760 m/sec. Grid spacing is 1°; latitude and longitude of left upper corner of each map are 43° N and 26° E.

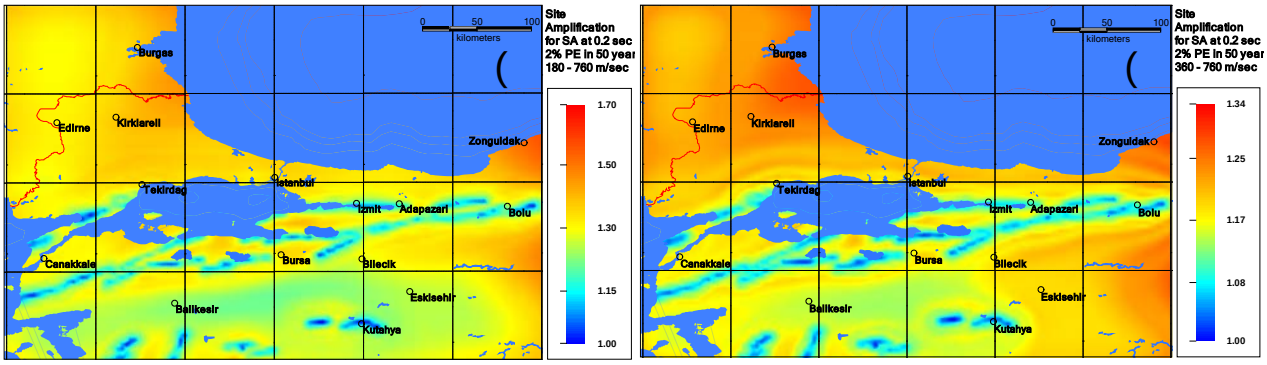

Fig. 9 - Site amplification map of the Marmara region for spectral acceleration (SA) at 0.2 sec for 2% probability of being exceeded in 50 years. Left panel shows ratio of ground motion estimate between V_{S30} = 180 m/sec and V_{S30} = 760 m/sec; right panel shows ratio of ground motion estimate between V_{S30} = 360 m/sec and V_{S30} = 760 m/sec. Grid spacing is 1°; latitude and longitude of left upper corner of each map are 43° N and 26° E.

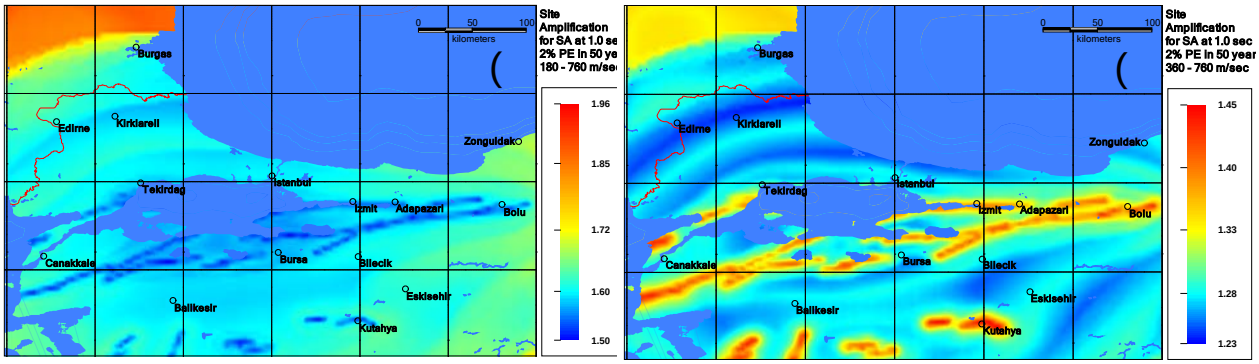

Fig. 10 - Site amplification map of the Marmara region for spectral acceleration (SA) at 1 sec for 2% probability of being exceeded in 50 years. Left panel shows ratio of ground motion estimate between V_{S30} = 180 m/sec and V_{S30} = 760 m/sec; right panel shows ratio of ground motion estimate between V_{S30} = 360 m/sec and V_{S30} = 760 m/sec. Grid spacing is 1°; latitude and longitude of left upper corner of each map are 43° N and 26° E.

5. Hazard: Determinism Based Estimates

Deterministic Seismic Hazard Analysis (DSHA) is based on the teaching that every event in the universe is caused and controlled by natural law, even though we do not quite know what law it is that nucleates earthquakes. It combines geological information and seismicity data to identify earthquake sources and to interpret the largest earthquake each source is capable of producing under the presently achieved state of knowledge or hypothetical tectonic activity with little or no regard of recurrence period. This is called Maximum Capable Earthquake (MCE), one that will presumably cause the most severe ground motions. The estimation of MCE is highly dicey because the chaotic and unstable processes in the earth's crust do not lend themselves to easy modeling. Conventional wisdom usually errs when one attempts to forecast what a particular fault will do within geological time spans. A drawback in DSHA is that, uncertainty in the state of knowledge is ignored.

I considered historical seismicity and the Wells and Coppersmith (1994) relation between the fault lengths and earthquake magnitudes. Using these details and the same suite of GMPEs weighted with the same consistent logic tree weight approach, the PGA and spectral acceleration values at 0.2 and 1 s were estimated.

Six plausible earthquake scenarios distilled from the information on Fig. 3 were defined for the greater Sea of Marmara area considering individual and multiple ruptures of the Islands, Mid-Marmara, Çınarcık, and Off-Tekirdağ fault segments. These scenarios are shown in Fig. 11, where the rupture length and expected

magnitudes (M_{max}) computed according to the historic seismicity and the expression in Wells and Coppersmith (1994) are marked. In these scenarios, selected fault segments are assumed to rupture in strike-slip mechanism along their entire length. Hypocenter location of earthquakes is not taken as a variable because the GMPEs selected utilize a specific distance definition either as the closest distance to the co-seismic rupture plane (R_{rup}) or as the closest distance to the surface projection of the causative fault (R_{jb}). Both distance measures are independent of the hypocenter location but they do depend on the fault geometry.

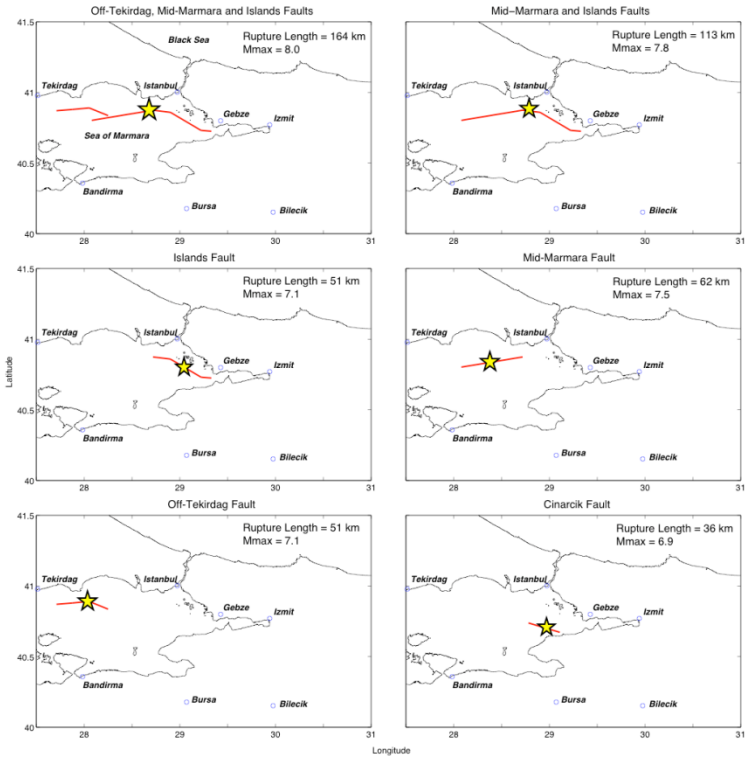

Fig. 11 - Six plausible earthquake scenarios defined for the greater Marmara area considering the individual and multiple rupturing of the Islands, Mid-Marmara, Çınarcık and Off-Tekirdağ fault segments. For each scenario, rupture length and expected magnitudes (M_{max}) are drawn from Wells and Coppersmith (1994).

The estimates of ground motion are drawn only from any one of the six fault ruptures in Fig. 11 all of which are under water. Faults on land that may also rupture are not pictured in this exercise. In Figures 12 through 14, the same set of ground motion parameters are mapped in scaled color.

6. Analysis and Discussion

For brevity, Fig. 12 shows only the median PGA. This map incorporates site effects by assigning a V_{S30} value corresponding terrain slope as proxy. PGA values, shown by the color gradient, indicate higher shaking level along the coastline of İstanbul, where Off-Tekirdağ, Mid-Marmara and Islands faults are about 10-15 km offshore. Multiple rupturing of these fault segments is expected to shake the coastal districts of the city in the European side with a PGA of 0.5 – 0.7 g. Intense PGA levels are also expected at the Istanbul Strait where it opens to the Sea of Marmara. The level of shaking gradually diminishes toward the north. The median PGA ranges between 0.4 g and 0.6 g at the coastal districts of the city in the Asian side. The estimated PGA increases to as much as 0.65 g at Adalar district (falsely called Prince's Islands). This table shows that the largest expected spectral acceleration at short periods (0.2-0.3 sec) that are close to the fundamental vibration period of 3- and 4-story reinforced concrete buildings is close to 1 g along the shoreline to the west of Istanbul, and at Sea of Marmara islands. The majority of the building stock in these parts of the city are 3-5 story in height, which are

the most vulnerable. At the city's financial district, which has mostly mid- and high-rise buildings (10-story to 40+

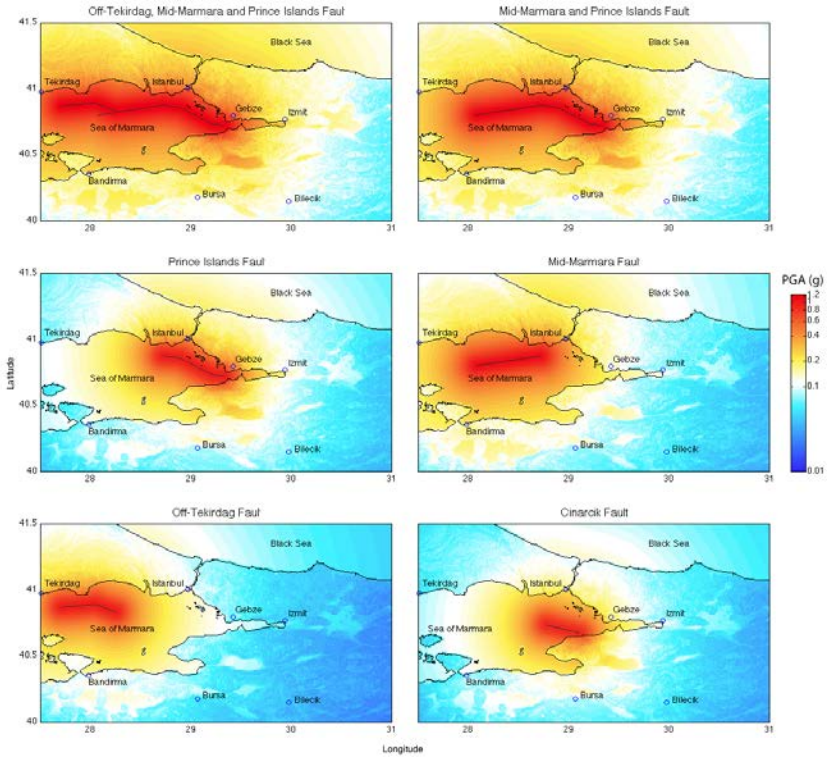

Fig. 12 - Peak ground acceleration (PGA) estimates for the Sea of Marmara region based on six different fault rupture scenarios.

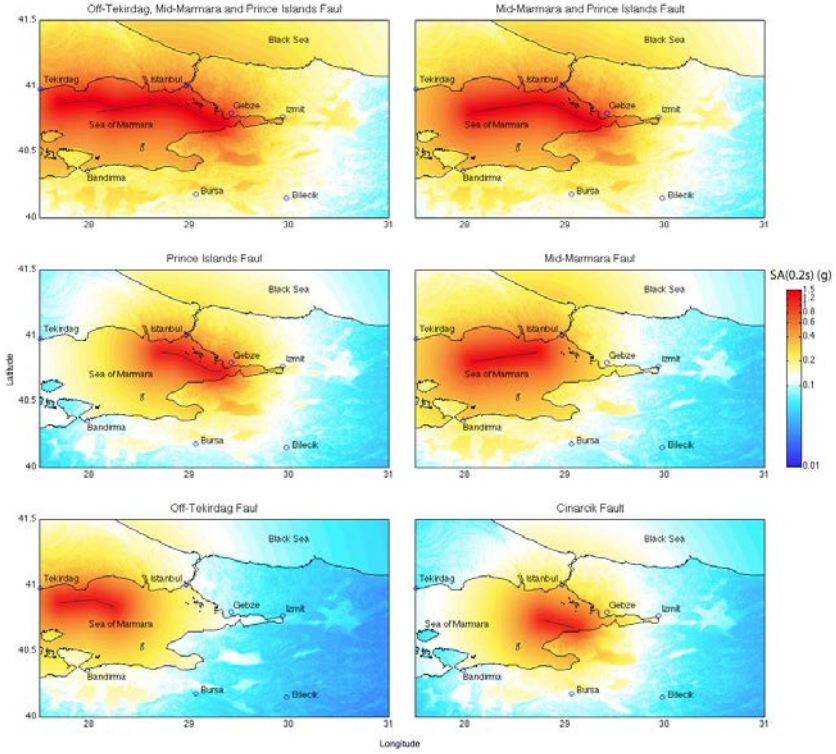

Fig. 13 - Estimates of 5%-damped spectral acceleration (SA) at 0.2 sec for the Sea of Marmara region based on six different fault rupture scenarios.

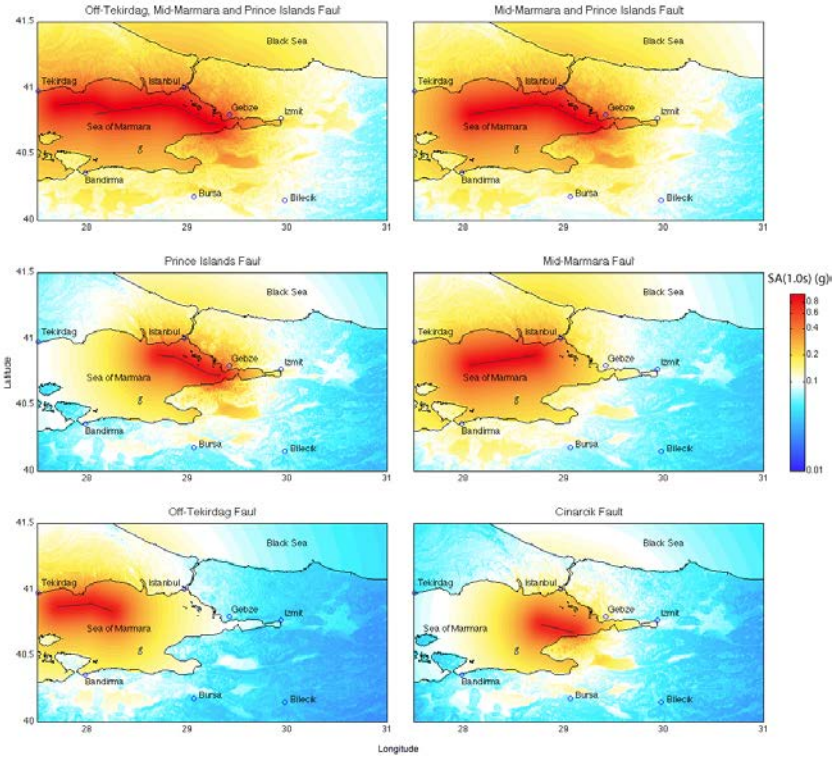

Fig. 14 - Estimates of 5%-damped spectral acceleration (SA) at 1 sec for the Sea of Marmara region based on six different fault rupture scenarios.

story), the largest expected spectral acceleration at 0.5, 1 and 3 s are 0.24, 0.2 and 0.07 g, respectively. This level of shaking indicates that the financial district of the city will be shaken with less intensity than its shoreline.

The overall agreement between the two sets of computations is noteworthy. Of course, no one-to-one agreement is possible because the fundamental approach in each method is different.

7. Acknowledgements

Dr. Erol Kalkan has provided timely material during the preparation of this paper. This is gratefully acknowledged.

8. References

[1] Ambraseys, N.N. (2009): *Earthquakes in the Mediterranean and Middle East*, Cambridge University Press.

[2] Armijo, R., B. Meyer, S. Navarro, G. King, and A. Barka (2002): "Asymmetric slip partitioning in the Marmara Sea pull-apart: a clue to propagation processes of the North Anatolian fault?", *Terranova* **14**: 80–86.

[3] Armijo, R. and 22 co-authors (2005): "Submarine fault scarps in the Sea of Marmara pull-apart (North Anatolian Fault): implications for seismic hazard in Istanbul," *Geochem. Geophys. Geosyst.* **6**(6): 1–29.

[4] Finkel, C.F. ve N. N. Ambraseys (1997): "The Marmara Sea earthquake of 10 July 1894 and its effects on historic buildings", *Anatolia Moderna [Yeni Anadolu]*, **VII**: 49-58.

[5] Griffiths, J.H.P., A. Irfanoğlu and S. Pujol (2007): "Istanbul at the threshold: an evaluation of the seismic risk in Istanbul," *Earthquake Spectra*, **23**(1): 63–75.

[6] Gülkan, P. (2013): "A dispassionate view of seismic hazard assessment," *Seismological Research Letters*, **84** (3): 413-416.

[7] Hubert-Ferrari, A. Barka, A.A. Jacquess, E. Nalbant, S.S. Meyer, B. Armijo, R. Tapponier, P. King, G.C.P. (2000): "Seismic hazard in the Marmara Sea following the Izmit earthquake," *Nature*, **404**: 269-272.

[8] Kalkan, E., P. Gülkan, N.Y. Öztürk and M. Çelebi (2009): "Re-examination of probabilistic seismic hazard in the Marmara Sea Region," *Bull. Seism. Soc. Am.*: **99** (4): 2127–2146.

[9] Le Pichon, X. and 11 co-authors (2001): "The active main Marmara fault," *Earth and Planetary Science Letters*, **192**: 595-616.

[10] Mazlum, D. (2003): "The earthquake of 22 May 1766 and its effects on the built environment in Istanbul," *İTÜ Journal: Architecture, Planning, Design*, **1**(1): 49-57.

[11] McClusky, S. and 27 coauthors, (2000): "Global Positioning System constraints on plate kinematics and dynamics in the eastern Mediterranean and Caucasus", *J. Geophys. Res.*, **105:** 5695-5719.

[12] Parsons, T., S. Toda, R.S. Stein, A. Barka, J. H. Dieterich (2000): "Heightened odds of large earthquakes near Istanbul: An interaction-based probability calculation," *Science*, (**288**): 661-665.

[13] Parsons, T. (2004): "Recalculated probability of M≥7 Earthquakes beneath the Sea of Marmara, Turkey. *Journal of Geophysical Research*, (**109**), B5304.

[14] Straub, C., Kahle, H-G., Schindler, C. (1997): "GPS and geologic estimates of the tectonic activity in the Marmara Sea region, NW Anatolia" *J. Geophys. Res.*, **102** (27); 587-601.

[15] Yenier, E., Erdoğan, O. and Akkar, S. (2008): "Empirical relationships for magnitude and source-to- site distance conversions using recently compiled Turkish strong-ground motion database," *Proc. 14th World Conference on Earthquake Engineering*, Oct. 12-17, Beijing.

[16] Gülkan, P. and Kalkan, E. (2002): "Attenuation modeling of recent earthquakes in Turkey," *Journal of Seismology*, **6(**3): 397-409.

[17] Kalkan, E. and Gülkan, P. (2004): "Site-dependent spectra derived from ground motion records in Turkey, *Earthquake Spectra*, **20(**4): 1111-1138.

[18] Kalkan, E. and Gülkan, P. (2004): "Empirical attenuation equations for vertical ground motion in Turkey, *Earthquake Spectra*, **20(**3): 853-882.

[19] Akkar, S. and 5 co-authors (2009): "The recently compiled Turkish strong motion database: preliminary investigation for seismological parameters," *Journal of Seismology*, **14**(3): 457-479.

[20] Campbell, K. and Bozorgnia, Y. (2008): "NGA ground motion model for the geometric mean horizontal component of PGA, PGV, PGD and 5% damped linear elastic response spectra for periods ranging from 0.01 to 10 s," *Earthquake Spectra*, **24(**1): 139-171.

[21] Boore, D. M. and Atkinson, G. (2008): "Ground-motion prediction equations for the average horizontal component of PGA, PGV, and 5%-damped PSA at spectral periods between 0.01 s and 10.0 s," Earthquake Spectra, **24(**1): 99-138.

[22] Chiou, B. and Youngs, R. (2008): "An NGA model for the average horizontal component of peak ground motion and response spectra," *Earthquake Spectra*, **24(**1): 173-215.

[23] Choi, Y. and Stewart, J.P. (2005): "Nonlinear site amplification as a function of 30 m shear wave velocity, *Earthquake Spectra*, **21**(1): 1–30.

[24] Wells, D.L. and Coppersmith, K.J. (1994): "New empirical relationships among magnitude, rupture length, rupture width, rupture area, and surface displacement," *Bull. Seism. Soc. Am.* (**84**)4: 974-1002.